Mechanism of *c*-axis orientation of $L1_0$ FePt in nanostructured FePt/B_2O_3 thin films

T. Ichitsubo,* S. Tojo, T. Uchihara, and E. Matsubara
Department of Materials Science and Engineering, Kyoto University, Kyoto 606-8501, Japan

A. Fujita
Graduate School of Engineering, Tohoku University, Sendai 980-8579, Japan

K. Takahashi and K. Watanabe
Institute for Materials Research, Tohoku University, Sendai 980-8577, Japan
(Received 17 October 2007; published 11 March 2008)

In oder to obtain a high-density magnetic recording medium using an $L1_0$ ferromagnetic ordered alloy, it is imperative to make its *c*-axis perpendicular to the thin film. In this work, we have investigated experimentally the *c*-axis orientation process of the $L1_0$ FePt in nanostructured FePt/B_2O_3 thin films, and its orientation mechanism is proposed on the basis of the micromechanics concept. From our present experimental results, we have found that there are three characteristic features when such *c*-axis orientation occurs in the thin films: the marked crystallographic orientation occurs during the cooling process, the axial ratio c/a experimentally observed tends to be considerably lower than the equilibrium value, and the degree of *c*-axis orientation is lowered for a relatively thick film, that is, the plane-stress state plays a key role to make the *c*-axis perpendicular to the film surface. In-plane (biaxial) tensile stresses are considered to be yielded due to the thermal shrinking difference between the two materials, and ordered FePt particles with the *c*-axis perpendicular to the film surface is considerably stabilized under such in-plane tensile stresses in terms of the mechanical interaction energy. The validity of this mechanism is also confirmed for CoPt/B_2O_3 thin films.

DOI: 10.1103/PhysRevB.77.094114 PACS number(s): 68.55.−a, 68.15.+e, 61.30.Gd

I. INTRODUCTION

Ferromagnetic $L1_0$ ordered alloys, FePt, CoPt, and FePd, are highly expected as forthcoming high-density recording materials, because they possess a large uniaxial magnetocrystalline anisotropy of $K \sim 10^6$ J/m^3, where the *c* axis is the easy axis of the magnetization.[1] Hence, they have an excellent potential to yield high coercivity H_c, and such a large K enables reduction of the size of magnetic particles down to several nanometers without being superparamagnetic in terms of the KV/k_BT criterion. From both of the technological and scientific importance, extensive efforts have been made to fabricate FePt, CoPt, and FePd thin films with various techniques, e.g., the chemical solution process,[2,3] molecular beam epitaxy,[4] electron beam evaporation,[5,6] and ion beam or magnetron sputtering.[7–9]

For high-density magnetic recording media, it is preferred that the nanoparticles are isolated and regularly arrayed. Several years ago, a prominent work has been reported by Sun *et al.*;[2] they showed that self-assembled nanoparticles can be fabricated by a chemical reaction (thermal decomposition and reduction of organometallic compounds), and the numerous nanoparticles are regularly arrayed in the triangle or tetragonal lattices. However, since the self-assembled nanoparticles have a disordered fcc structure, the heat treatment for the $L1_0$ ordering is required to obtain the large coercivity of thin films, which leads to collapse of the regular arrangement of nanoparticles.[3] Recently, to overcome this problem, a novel method to synthesize fully ordered FePt nanoparticles has been reported by Yamamoto *et al.*[10] In this method, high-melting-temperature SiO_2 is covered by isolated FePt nanoparticles prepared by the method of Sun *et al.*, and subsequently the SiO_2 covered nanoparticles are annealed at a sufficiently high temperature for fully ordering reaction and extracting its high coercivity. On the other hand, as a method of controlling the *c*-axis orientation of $L1_0$ ordered alloys, one can choose an epitaxial-like growth method by utilizing an appropriate substrate.[11–14] Shima *et al.* have shown a very excellent magnetic coercivity (105 kOe at 4.5 K and 70 kOe at room temperature) of FePt nanoparticles epitaxially grown on a MgO substrate.[11] Besides, it has been claimed that the difference in the thermal expansion coefficients between FePt or CoPt and a substrate plays a significant role of the *c*-axis orientation of $L1_0$ alloys.[12–15]

Further interestingly, the *c* axis of FePt has been shown to be oriented in the normal direction of the film surface with the aid of B_2O_3 interlayers.[16,17] However, in some case, the *c*-axis orientation cannot be attained despite the similar FePt/B_2O_3 multilayered films.[18] In those works, the thin films were annealed at 550 °C, which is above the melting temperature T_m of B_2O_3 ($T_m \sim 450$ °C).[19] It is quite mysterious and fascinating that the *c*-axis orientation seemingly occurs in the molten B_2O_3, and the *c*-axis orientation mechanism is still unclear to date. In this paper, we focus those intriguing works[16–18] to elucidate the mechanism of the *c*-axis orientation of FePt particles experimentally and phenomenologically. In an FePd single-crystal bulk alloy, our previous work has shown that the *c*-axis orientation can be controlled by applying a magnetic field or compressive stress,[20–23] that is, the monovariant ordered structure is formed under such external fields. On this basis, taking notice of in-plane (biaxial) tensile stresses that may be yielded by the difference in the thermal shrinking between FePt and B_2O_3 after accommodation to FePt nanoparticles of the molten B_2O_3, we propose a mechanism of the *c*-axis orientation of $L1_0$ ordered FePt existing in B_2O_3 layers. The validity of

the mechanism proposed here is further examined for $CoPt/B_2O_3$ multilayered thin films. In addition, we have investigated a fabrication method of isolated FePt or FePd nanoparticles dispersed on a Si substrate by utilizing a magnetic field,[24,25] because a magnetic field is considered to have a high potential for controlling the thin film structure. Also in this work, we have performed heat treatments under a magnetic field, and its effects are described briefly in Sec. III.

II. EXPERIMENT

Thin films were prepared on Si(100) substrates by using a three-cathode magnetron sputtering apparatus with Fe (or Co), Pt, and B_2O_3 targets of 2-in. diameter; rf (13.56 MHz) sputter depositions were performed at room temperature in an Ar (purity: 99.99%) atmosphere of about 0.3 Pa, after the base pressure reached about 10^{-5} Pa. In order to obtain uniform-thickness thin films, substrates were let be rotated at 12°/s during deposition and the distance between the cathodes and a substrate was set at 200 mm as long as possible. The sputtering rates of Fe/Pt (cathode power: 120 W/50 W), Co/Pt (100 W/58 W), and B_2O_3 (100 W) in our apparatus were 16.5, 13.9, and 90.2 s/nm, respectively. We have prepared three types of thin films: (i) multilayered thin films $(3\ \text{nm}\ B_2O_3/3\ \text{nm}\ \text{FePt})_{10}$ and $(3\ \text{nm}\ B_2O_3/3\ \text{nm}\ \text{CoPt})_{10}$, (ii) thick films, 30 nm B_2O_3/30 nm FePt/30 nm B_2O_3, and (iii) triple-layer thin films, 3 nm B_2O_3/5 nm FePt/3 nm B_2O_3. Atomic concentrations of Fe/Pt and Co/Pt of the prepared thin films were measured by the energy dispersion x-ray spectroscopy; they are 52/48 and 53/47, respectively, being within the $L1_0$-compound forming concentrations.

Heat treatments were made in two kinds of furnaces: a differential scanning calorimetry (DSC) furnace (PerkinElmer: diamond DSC) in a N_2 atmosphere and a high-magnetic-field furnace[26] (High Field Laboratory for Superconducting Materials, Institute for Materials Research, Tohoku University) in an Ar-5%H_2 atmosphere. The former was used for a rapid cooling treatment after isothermal annealing (it is possible to cool down at 500 °C/min in the DSC furnace) and also for making the annealing temperature accurate, and the latter was employed for the heat treatment under a magnetic field of 100 kOe (10 T), where a magnetic field was applied along the direction normal to the substrate surface.

The crystallographic orientation of the postannealed thin films was analyzed by the x-ray diffraction method using Mo $K\alpha$ radiation and the surface morphologies were observed by field-emission scanning electron microscopy (FESEM) (JEOL JSM-6500F). The superconducting quantum interference device (SQUID) (Quantum Design) with a field of up to 50 kOe (5 T) was used to measure the hysteresis curves at room temperature.

III. RESULTS

A. Annealing without a magnetic field

The prepared multilayered thin films, $(3\ \text{nm}\ B_2O_3/3\ \text{nm}\ \text{FePt})_{10}$, were annealed at 450, 550 °C for 1 h, and 700 °C for 3 h in the DSC furnace (without a magnetic field); each heat treatment was done on each fresh sample. The long-time annealing at such a high temperature (3 h, 700 °C) was performed to let the ordering proceed sufficiently. The annealing temperature of 450 °C is close to the melting temperature of B_2O_3 (Ref. 19) and below the Curie temperature of FePt ($T_C \sim 480$ °C). Figure 1(a) shows the x-ray diffraction (XRD) profiles. The as-deposited thin film and annealed thin film at 450 °C showed only the (111) diffraction peak, which means that these thin films have a 111 texture. In contrast, the thin films annealed at 550 and 700 °C exhibited the (001) superlattice diffraction. Especially, the $L1_0$ c axis of the thin film annealed at 550 °C is found to be mostly oriented along the normal direction of the thin film. However, the degree of orientation of the thin film annealed at 700 °C was lower compared to the former thin film, which can be judged from the existence of the (111) diffraction. Thus, when the thin film is annealed at a relatively high temperature where the ordering reaction sufficiently proceed, the degree of c-axis orientation tends to be lowered. It should be noted here that the crystallographic c axis has been oriented in the perpendicular direction of the thin film surface without a magnetic field. Figure 1(b) shows

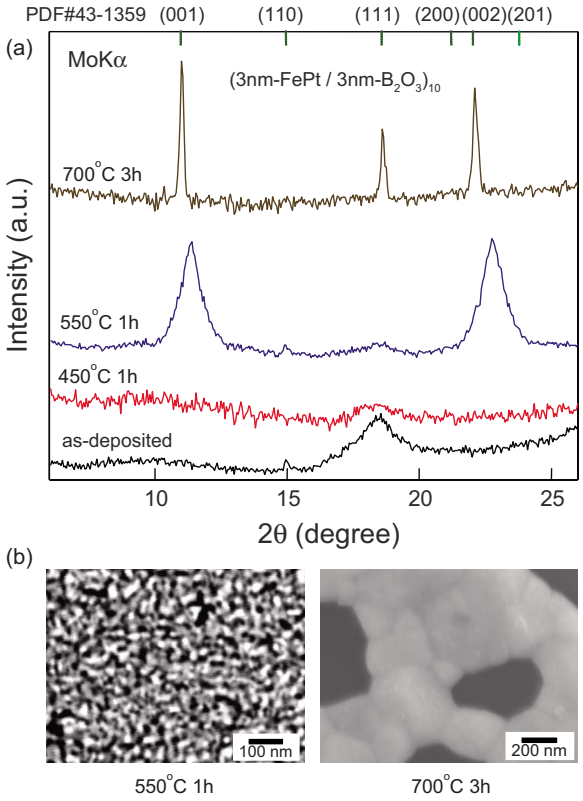

FIG. 1. (Color online) (a) XRD profiles of $(3\ \text{nm}\ B_2O_3/3\ \text{nm}\ \text{FePt})_{10}$ thin films obtained for various annealing temperatures, and (b) FESEM micrographs. The c-axis orientation of $(3\ \text{nm}\ B_2O_3/3\ \text{nm}\ \text{FePt})_{10}$ is lowered when the annealing temperature is relatively high (700 °C). In contrast, the crystallographic orientation hardly occurs for the thin film annealed at 450 °C. The annealing temperature of 550 °C is the most appropriate for the c-axis orientation and the enhancement of ordering.

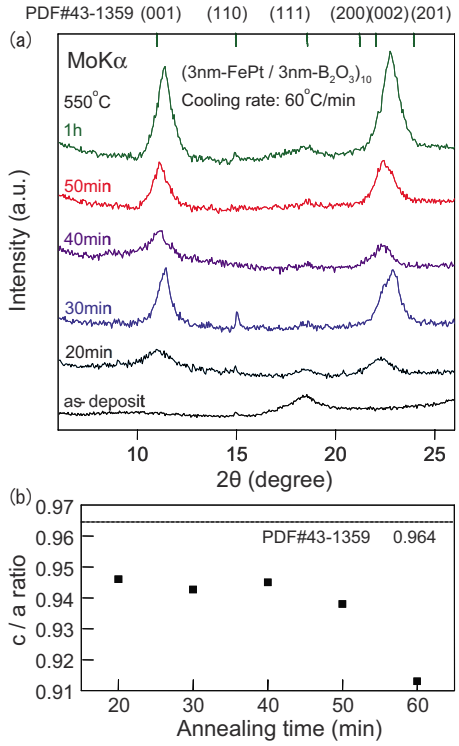

FIG. 2. (Color online) (a) XRD profiles of (3 nm B_2O_3/3 nm FePt)$_{10}$ thin films obtained for various annealing times, and (b) the axial ratio c/a obtained from (002) and (111) diffractions. The experimental c/a values are considerably smaller than the equilibrium value 0.964 (PDF No. 43-1359).

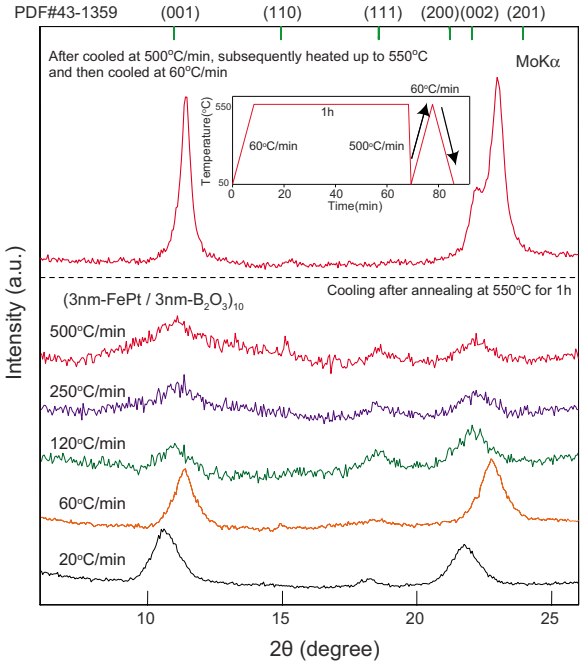

FIG. 3. (Color online) XRD profiles obtained for the multilayered thin films, (3 nm B_2O_3/3 nm FePt)$_{10}$, that were cooled down at various cooling rates after annealed at 550 °C for 1 h. The heating rate to the objective temperature was set at 60 °C/min in all cases. Despite the same annealing time, degree of the c-axis orientation is very different. The top XRD profile was obtained for the thin film that was again heated and cooled at 60 °C/min after cooled at 500 °C/min (after annealed at 550 °C for 1 h). Remarkable c-axis orientation is found to occur in the subsequent slow cooling (60 °C/min) process.

the FESEM micrographs of the thin films annealed at 550 and 700 °C. Apparently, FePt domains in the thin film of 550 °C tend to be aggregated but FePt particles of nanometer scale were still isolated, but in contrast the 700 °C thin film exhibited completely aggregated structure. This difference in the structures is responsible for the sharpness and broadening of the XRD peaks.

Figure 2(a) presents the XRD profiles as a function of the annealing time. All the thin films were annealed at 550 °C and subsequently cooled down to room temperature at 60 °C/min. Although the ordering in the thin film annealed for 20 min seems not to progress (but c-axis orientation is attained), the ordering in the other thin films greatly proceeds and their c axes are virtually oriented to the normal direction of the film surface. In addition, the progress degree of the ordering appears to be not so dependent on the annealing time. Figure 2(b) shows the c/a ratio determined from the (111) and (002) fundamental diffractions. All the obtained c/a ratios underrun the reported value, 0.964, in the powder diffraction file (PDF No. 43-1359), indicating that the a axis of the $L1_0$ lattice is markedly stretched, probably, due to the elastic stress (discussed later).

Next, we have investigated the cooling-rate dependence of the c-axis orientation. The thin films were cooled down to room temperature at 20–500 °C/min after annealed at 550 °C for 1 h; in all the heat treatments, the heating rate was coordinated to be 60 °C/min. As found from Fig. 3, both 001 and 002 maximum intensities decrease and peaks spread when the cooling rate increases. A larger orientation distribution and size distribution lead to smaller intensities in the reciprocal direction scanned by the θ-2θ XRD. Thus, it is found that, despite the same annealing time of 1 h at 550 °C, as the cooling rate is higher, the degree of c-axis orientation becomes lower. Moreover, a subsequent heat treatment of slow heating and cooling at 60 °C/min was performed by using the thin film cooled at 500 °C/min after annealing at 550 °C for 1 h. By this heat treatment, the ordering is found to proceed significantly and the degree of c-axis orientation increases markedly although also the (200) peak appears weakly (see the top figure in Fig. 3). The axial ratio c/a roughly estimated from (001) and a faint peak of (110) diffraction peaks is approximately 0.945, being considerably smaller than the equilibrium value, 0.964, also in this case. Thus, it is found that the c-axis orientation occurs rather during the cooling process than during the isothermal annealing process. In addition, it should be noted that the XRD profile for the slow cooling process at 20 °C/min is close to the standard profile (PDF No. 43-1359) given in powder diffraction files.

We have also examined how the c-axis orientation alters when the thickness of thin film increases. Figure 4 shows the XRD profile of the relatively thick film, 30 nm B_2O_3/30 nm FePt/30 nm B_2O_3, after annealed at 550 °C for 1 h. Since only the (111) peak is visible, it is difficult to judge to what

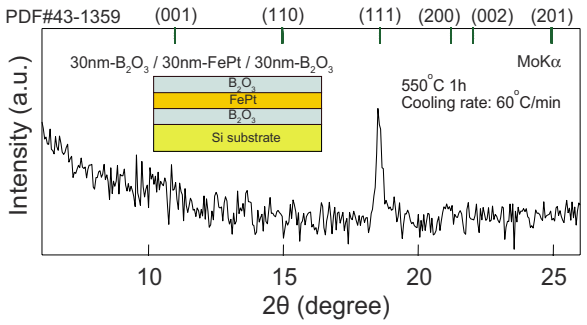

FIG. 4. (Color online) XRD profile obtained for the triple-layered relatively thick film, 30 nm B_2O_3/30 nm FePt/30 nm B_2O_3, annealed at 550 °C for 1 h. The (111) diffraction peak was only detected in such a thick film.

degree the ordering progresses. Thus, it is found that the *c*-axis orientation does not occur when the thickness of thin film increases, which is consistent with the results reported previously.[18]

B. Annealing under a magnetic field

The multilayered thin films, (3 nm B_2O_3/3 nm FePt)$_{10}$, were annealed under a magnetic field of 100 kOe at 450 °C for 1 and 12 h and 550 °C for 1 h; the cooling rate was set at 10 °C/min (but the rate becomes slower below 300 °C, and this is the constraint on the apparatus and very different from the DSC furnace). Figure 5(a) shows the XRD profiles of the thin films subjected to various heat treatments. When the thin film was annealed at 450 °C, the (111) peak was dominant without regard to the annealing time. In contrast, in the case of 550 °C, the (001) superlattice and (002) fundamental diffractions indicate that the ordering proceeds sufficiently and the degree of *c*-axis orientation is very high. For reference, also a fresh sample was annealed without a magnetic field at 550 °C for 1 h. As shown in the previous section, the ordering and *c*-axis orientation can be attained without a magnetic field; this is consistent with the above-mentioned results obtained for the DSC furnace. Compared to the nonmagnetic annealing, however, the half bandwidth of the diffraction peaks for the thin film annealed under 100 kOe is clearly broader than that for the thin film without a magnetic field. The sizes of crystallites of the former and the latter are estimated with the Sherrer equation to be 8 and 18 nm, respectively. As seen in the FESEM micrograph in Fig. 5(b), FePt nanoparticles were isolated from each other, which seems to be different from the microstructure of the thin film annealed in the DSC furnace (compare to the FESEM micrographs in Fig. 1), in which the nanoparticles are spatially connected continuously. Thus, it is shown that magnetic particles tend to be isolated under a magnetic field, which may be caused by the repulsive force between the magnetic dipoles.[24] Also in this case, since the thin films were slowly cooled in the magnetic-field furnace, the XRD peak positions are close to the standard peak positions in the powder diffraction file (PDF No. 43-1359).

Figure 5(c) shows the *M*-*H* loop obtained for the thin films annealed at 450 and 550 °C for 1 h under 100 kOe.

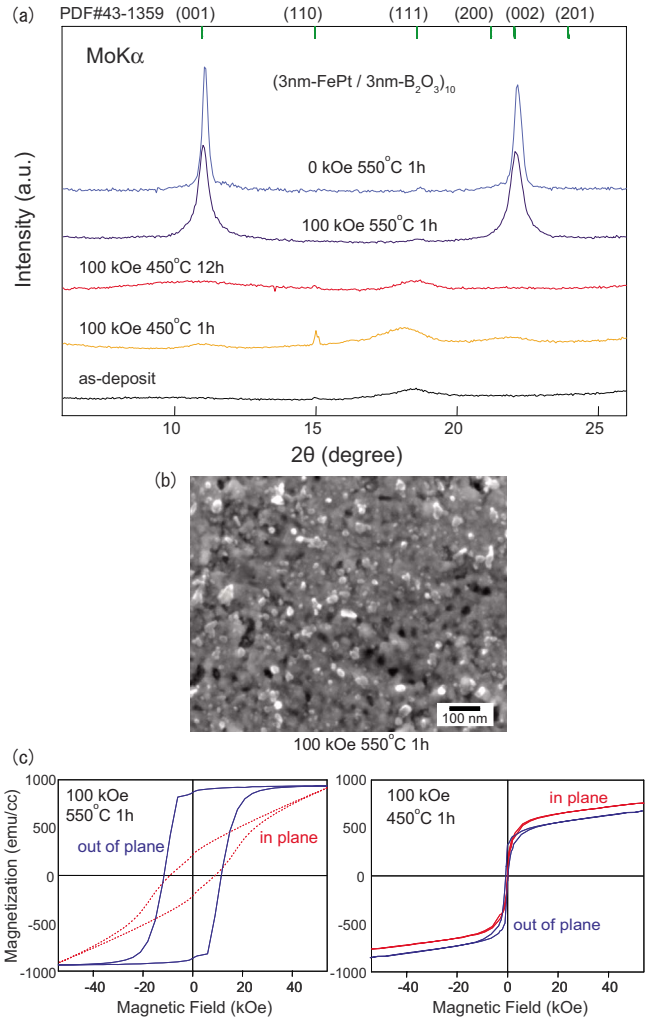

FIG. 5. (Color online) (a) XRD profiles obtained for the multilayered thin films, (3 nm B_2O_3/3 nm FePt)$_{10}$, annealed at 450 and 550 °C for 1 h with or without a magnetic field of 100 kOe. (b) FESEM micrograph of the thin film annealed at 550 °C for 1 h. (c) *M*-*H* loop measured by a SQUID for the thin films annealed at 550 °C (left) and 450 °C (right).

The coercivity of the thin film of 450 °C is quite small, exhibiting a soft magnetic property. In contrast, since the thin film of 550 °C is fully ordered and its *c* axis is oriented in the normal direction of the film surface, it shows the magnetocrystalline anisotropic behavior and the coercivity H_c of "out of plane" is about 12 kOe. However, H_c of "in plane" is also large; this is probably due to the existence of the domains with the *c* axis in plane to no small extent. Shima *et al.* have reported that the epitaxial FePt nanoparticles on a MgO substrate show a very high coercivity of 70 kOe at room temperature.[11] The present lower value of H_c=12kOe is considered to be ascribed to the coarsening of particles to about 20 nm in diameter. In order to enhance H_c, it is needed to reduce the size of nanoparticles down to a single nanometer scale.

Figure 6(a) shows the XRD profiles of the triple-layer thin films, 3 nm B_2O_3/5 nm FePt/3 nm B_2O_3, annealed at 550 °C for 1 h with or without a magnetic field of 100 kOe.

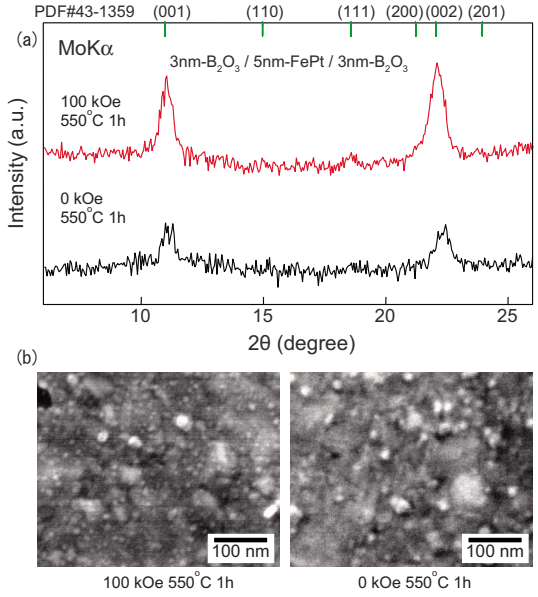

FIG. 6. (Color online) (a) XRD profiles obtained for the triple-layered thin films, 3 nm B_2O_3/5 nm FePt/3 nm B_2O_3, annealed at 550 °C for 1 h with or without a magnetic field of 100 kOe and (b) FESEM micrographs for the respective samples.

In both cases, numerous isolated nanoparticles are found to be dispersed on the Si substrate in Fig. 6(b). The ordering reaction of the thin film annealed under a magnetic field of 100 kOe appears to progress more rapidly compared to the film annealed without a magnetic field; this trend is consistent with a previous work by Wang *et al.*[27] Furthermore, the size of nanoparticles of the thin film annealed with 100 kOe seems to be slightly smaller than that without a magnetic field. In both cases, the c axis tends to become normal to the film surface, and this tendency is the same as the multilayered films.

IV. DISCUSSION

Our present experimental results have shown the promotion of the ordering kinetics and the remarkable c-axis orientation of FePt/B_2O_3 thin films. We can be aware that there are three characteristic features when such c-axis orientation occurs in the thin films. (I) As seen in Figs. 2 and 3, the crystallographic rotation (or orientation) occurs during the cooling process rather than the isothermal annealing at 550 °C. (II) The axial ratio c/a experimentally observed tends to be considerably lower than the equilibrium value (although it tends to become close to the equilibrium value when it is cooled slowly, e.g., at 10–20 °C/min). (III) Moreover, the degree of c-axis orientation cannot be attained for a relatively thick film such as 30 nm B_2O_3/30 nm FePt/30 nm B_2O_3, that is, the plane-stress state plays a key role to make the c-axis perpendicular to the film surface. On the basis of these present results, we here discuss the mechanism of the c-axis orientation from the viewpoint of the elastic stress caused by the difference in the thermal shrinking between FePt and B_2O_3.

First, we estimate a magnitude of a tensile stress applied to FePt particles on the basis of the c-axis-oriented nanostructures obtained in the experiments. On the assumption of no volume change accompanied by the ordering transformation from fcc to $L1_0$, i.e., $(1+\epsilon^*)^2(1-2\epsilon^*)\approx 1$, the tetragonal distortion ϵ^* in a stress-free "equilibrium" state measured from the mother cubic phase is written as

$$\epsilon^*_{\mathrm{eq}} \approx \tfrac{1}{3}[1-(c/a)_{\mathrm{eq}}]. \tag{1}$$

In this stress-free state, the tetragonal distortion is estimated to be $\epsilon^*_{\mathrm{eq}} \approx 0.012$ by using the axial ratio, $(c/a)_{\mathrm{eq}}$, obtained from the powder diffraction file (PDF No. 43-1359). As stated above, however, the present experimental axial ratios, $(c/a)_{\mathrm{expt}}$, is considerably small, which indicates that FePt nanoparticles are elastically strained by some reason. Here, we shall evaluate the elastic strain and stress caused under *the plane-stress condition*

$$\sigma_3 = 2c_{12}\epsilon_a + c_{11}\epsilon_c = 0, \tag{2}$$

where ϵ_a and ϵ_c are, respectively, the elastic strains along the a axis and along the c axis, the subscripts 1, 2, and 3 are assigned for the in-plane directions and out-of-plane direction of a thin film, and c_{ij} denote the elastic constants of FePt. From Eq. (2), the experimental axial ratio $(c/a)_{\mathrm{expt}}$ can be expressed as

$$(c/a)_{\mathrm{expt}} = \frac{1-2\epsilon^*_{\mathrm{eq}} - (2c_{12}/c_{11})\epsilon_a}{1+\epsilon^*_{\mathrm{eq}} + \epsilon_a}. \tag{3}$$

Hence, ϵ_a is expressed as

$$\epsilon_a = \frac{1-2\epsilon^*_{\mathrm{eq}} - (1+\epsilon^*_{\mathrm{eq}})(c/a)_{\mathrm{expt}}}{(c/a)_{\mathrm{expt}} + 2c_{12}/c_{11}}, \tag{4}$$

and the in-plane stresses σ_1 and σ_2 are given by

$$\sigma_1 = \sigma_2 = (c_{11}+c_{12})\epsilon_a + c_{12}\epsilon_c. \tag{5}$$

Here, since the data of the elastic constants of FePt are unavailable, we tentatively assume that the elastic constants of ordered and disordered FePt are equal to the single-crystal elastic constants of an fcc disordered FePd (c_{11}=215, c_{12}=161, and c_{44}=83 GPa).[29] Since $(c/a)_{\mathrm{expt}}$ is approximately 0.945 as shown in Fig. 2, the elastic strain and in-plane stresses are estimated to be

$$\epsilon_a \approx 0.008, \quad \epsilon_c \approx -0.012, \quad \sigma_1 = \sigma_2 \approx 1100\ [\mathrm{MPa}].$$

Thus, it is found from the present analysis based on the experimentally obtained c/a ratio that considerably large tensile stresses are being applied to the FePt nanoparticles.

Suppose that the in-plane stresses obtained above have a feature of an external stress field (i.e., the B_2O_3 matrix has a potential to yield fixed biaxial tensile stresses against FePt particles). Here, we consider two cases: formation of ordered nanoparticles (A) with the c axis perpendicular to the film surface (termed [001] particles), and (B) with the c axis parallel to the film surface (termed [100] particles). Then, the elastic strain energy can be calculated as

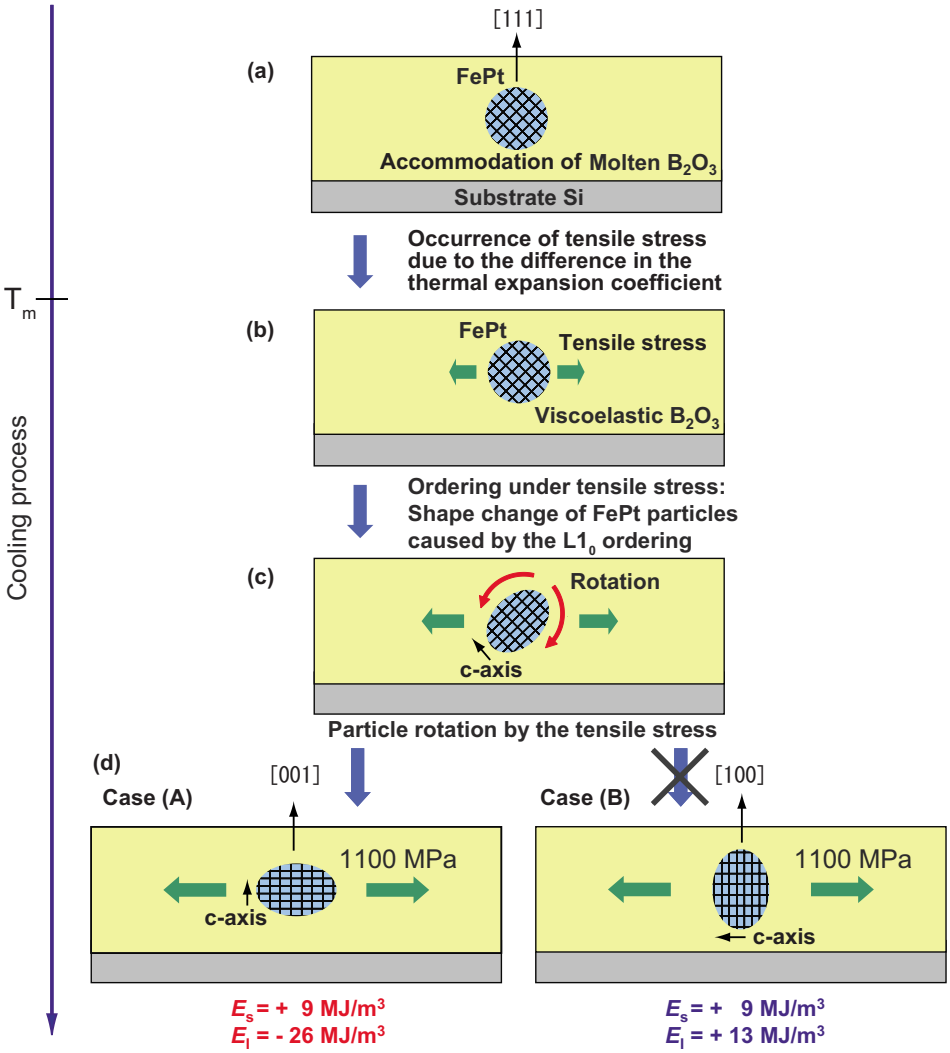

FIG. 7. (Color online) Schematic illustration showing the mechanism of the *c*-axis orientation upon cooling process. (a) Accommodation of molten B_2O_3 to FePt nanoparticles. (b) Occurrence of tensile stress due to the thermal shrinking difference between FePt and B_2O_3. (c) Macroscopic shape change of FePt particles due to the tetragonal distortion and rotation of particles caused by ordering under the tensile stress. (d) Preferable rotation of the ordered FePt nanoparticle.

$$E_s = \frac{1}{2}\sum_i \sigma_i \epsilon_i, \tag{6}$$

where $\epsilon_i = (\epsilon_a, \epsilon_a, \epsilon_c, 0, 0, 0)$ in case (A). The strain energy E_s thus estimated is about 9 MJ/m^3. Also when the [100] particles are formed under in-plane tensile stresses of 1100 MPa [case (B)], the strain energy becomes equal to the above value, because the elastic strains are completely the same as those in case (A) due to the assumed cubic symmetry of elastic constants.[30] Therefore, we cannot discuss the *c*-axis orientation only in terms of the strain energy. As to the selection of the [100] or [001] particles, the difference in the two cases (A) and (B) is yielded by the term of the mechanical interaction energy, in other words, the potential energy of the external load. The mechanical interaction energy E_I can be estimated in the micromechanics theory[28]

$$E_I = -\sum_i \sigma_i \epsilon_i^*, \tag{7}$$

where $\epsilon_i^* = (\epsilon_{eq}^*, \epsilon_{eq}^*, -2\epsilon_{eq}^*, 0, 0, 0)$ in case (A) and $\epsilon_i^* = (-2\epsilon_{eq}^*, \epsilon_{eq}^*, \epsilon_{eq}^*, 0, 0, 0)$ in case (B). The mechanical interaction energy E_I is estimated to be about −26 MJ/m^3 for the [001] particles (*c* axis ⊥ film surface), and 13 MJ/m^3 for the [100] particles (*c*-axis ∥ film surface). Incidentally, for the particles oriented in the [111] direction ([111] ⊥ film surface; the initial state of particles in the as-deposited films), the strain energy E_s is approximated to be 4 MJ/m^3 under $\sigma_1 = \sigma_2 \approx 1100$ [MPa], and the mechanical interaction energy E_I is rigorously calculated to be $E_I = 0$. Thus, we reach a conclusion that the particles with the *c* axis perpendicular to the film surface are the most preferred in terms of the total mechanical energy $E_s + E_I$.

Figure 7 summarizes schematically the mechanism of the *c*-axis orientation upon cooling process. When the thin films are heated up to 550 °C, B_2O_3 layers become soft and fluidic because the annealing temperature is higher than T_m of B_2O_3. Consequently, at such a temperature, B_2O_3 is considered to be accommodated to particlized FePt oriented in the [111] direction [Fig. 7(a)]. Upon subsequent cooling, B_2O_3 becomes solidified or highly viscoelastic state (it is known that B_2O_3 is a strong glass-forming material, frequently becomes glassy state below T_m by itself, and its viscosity is quite large).[19] Due to the difference in the thermal shrinking between the two substances, it is considered that in-plane (biaxial) tensile stresses are yielded [Fig. 7(b)]. Here it should

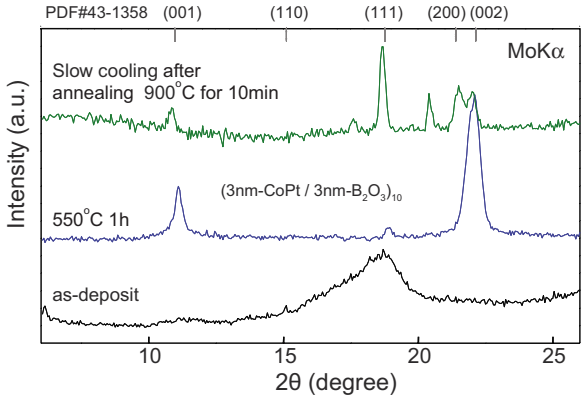

FIG. 8. (Color online) XRD profiles obtained for CoPt multilayered thin film, (3 nm B_2O_3/3 nm CoPt)$_{10}$. In the as-deposited film, the crystallographic [111] direction is oriented in the normal direction of the surface. The c-axis orientation occurs when the thin film is annealed at 550 °C, but in contrast, it does not occur when cooled down from 900 °C.

be noted that a plane-stress condition holds when the thickness of films is very small. When the ordering occurs under such tensile stresses, the macroscopic shape of the FePt nanoparticles is changed accompanied by the occurrence of the tetragonal distortion [Fig. 7(c)] and they are rotated and selectively oriented in the [001] direction in terms of minimization of the total mechanical energy [Fig. 7(d)].

The origin of the elastic strain will be explained in terms of the difference in the thermal expansion coefficient between FePt and B_2O_3. In general, thermal expansion coefficients of metals or alloys are of the order 10^{-5}/K and, in contrast, those of oxide glasses are of the order $10^{-6} \sim 10^{-7}$/K (e.g., SiO_2 glass or Pyrex glass).[15] If the difference in the thermal expansion coefficient is assumed to be of the order 10^{-5}/K, the elastic strain caused by the cooling of about 400 K from T_m of B_2O_3 to room temperature is roughly estimated to be of the order 10^{-3}. Thus, the order of the elastic strain due to the difference in their thermal expansion coefficients is consistent with that calculated on the basis of the experimental results.

Finally, in order to reveal universality of this mechanism, we tried to make an application to CoPt/B_2O_3 thin films. CoPt alloy is also an $L1_0$ ordered alloy exhibiting a large magnetocrystalline anisotropy and having a tetragonal axial ratio less than unity (c/a=0.973: PDF No. 43-1358). If the above mechanism is valid, a similar phenomenon associated with the c-axis orientation is expected to occur. Then, we have examined this event with multilayered thin film, (3 nm B_2O_3/3 nm CoPt)$_{10}$. Figure 8 shows XRD profiles obtained for (3 nm B_2O_3/3 nm CoPt)$_{10}$ thin films cooled down at 60 °C/min after annealed at 550 °C for 1 h and cooled down from 900 °C. Similarly, the c-axis orientation occurs for the thin film cooled down after annealed at 550 °C, but it does not take place for the thin film cooled slowly from 900 °C. During the cooling process from such a high temperature, the ordering reaction is considered to proceed sufficiently before the elastic-strain effect appears below T_m of B_2O_3. It is significant that the elastic-strain effect appears in the stage of the ordering reaction. Thus, the above-mentioned mechanism is found to be reasonable and may be valid for the other kinds of materials exhibiting a cubic-to-tetragonal phase transformation.

V. CONCLUSIONS

In this work, we have investigated the c-axis orientation mechanism of FePt nanoparticles in FePt/B_2O_3 thin films. From our present experimental results, we have found that there are three characteristic features when the c-axis orientation occurs in the thin films.

(1) The marked crystallographic rotation and/or orientation of the ordered particles occurs during cooling process rather than during isothermal annealing.

(2) The axial ratio c/a experimentally observed tends to be considerably lower than the equilibrium value, which indicates that in-plane (biaxial) tensile stresses are applied to FePt nanoparticles.

(3) The degree of c-axis orientation is lowered for a relatively thick film, namely, the plane-stress state plays a key role to make the c-axis perpendicular to the film surface.

Based on these results, we have discussed the mechanism of the c-axis orientation with the aid of the micromechanics concept. The in-plane tensile stresses are considered to be yielded due to the difference in the thermal shrinking between FePt and B_2O_3 in the cooling process after accommodation of B_2O_3 to FePt particles above T_m of B_2O_3. Under such in-plane (biaxial) tensile stresses, the FePt particles with the c axis parallel to the normal direction of the film surface are the most stabilized. The validity of this mechanism is also confirmed for CoPt/B_2O_3 thin films. Thus, using the low-melting-temperature materials as under- or interlayers and utilizing effectively the thermal expansion and/or shrinking difference after sufficiently adjusted and/or accommodated to the objective nanoparticles are significantly important to control the crystallographic orientation and to design the nanostructure of thin films. This mechanism is expected to be applicable to a wide range of materials possessing a crystallographic anisotropy.

ACKNOWLEDGMENT

The heat treatments under a magnetic field were performed at the High Field Laboratory for Superconducting Materials, Institute for Materials Research, Tohoku University.

*tichi@mtl.kyoto-u.ac.jp

[1] T. Klemmer, D. Hoydick, H. Okumura, B. Zhang, and W. A. Soffa, Scr. Metall. Mater. **33**, 1793 (1995).
[2] S. Sun, C. B. Murray, D. Weller, L. Folks, and A. Moser, Science **287**, 1989 (2000).
[3] J. W. Harrella, S. Wang, D. E. Nikles, and M. Chen, Appl. Phys. Lett. **79**, 4393 (2001).
[4] R. F. C. Farrow, D. Weller, R. F. Marks, M. F. Toney, S. Hom, G. R. Harp, and A. Cebollada, Appl. Phys. Lett. **69**, 1166 (1996).
[5] B. Bian, K. Sato, Y. Hirotsu, and A. Makino, Appl. Phys. Lett. **75**, 3686 (1999).
[6] K. Sato, B. Bian, and Y. Hirotsu, Jpn. J. Appl. Phys., Part 2 **39**, L1121 (2000).
[7] D. H. Ping, M. Ohnuma, K. Hono, M. Watanabe, T. Iwasa, and T. Masumoto, J. Appl. Phys. **90**, 4708 (2001).
[8] Y. K. Takahashi, M. Ohnuma, and K. Hono, Jpn. J. Appl. Phys., Part 2 **40**, L1367 (2001).
[9] Y. Huang, H. Okumura, G. C. Hadjipanayis, and D. Weller, J. Magn. Magn. Mater. **242-245**, 317 (2002).
[10] S. Yamamoto, Y. Morimoto, T. Ono, and M. Takano, Appl. Phys. Lett. **87**, 032503 (2005).
[11] T. Shima, K. Takanashi, Y. K. Takahashi, and K. Hono, Appl. Phys. Lett. **85**, 2571 (2004).
[12] O. Ersen, V. Parasote, V. Pierron-Bohnes, M. C. Cadeville, and C. Ulhaq-Bouillet, J. Appl. Phys. **93**, 2987 (2003).
[13] D. Halley, B. Gilles, P. Bayle-Guillemaud, R. Arenal, A. Marty, G. Patrat, and Y. Samson, Phys. Rev. B **70**, 174437 (2004).
[14] M. Abes, O. Ersen, C. Meny, G. Schmerber, M. Acosta, J. Arabski, C. Ulhaq-Bouillet, A. Dinia, P. Panissod, and V. Pierron-Bohnes, J. Appl. Phys. **101**, 063911 (2007).
[15] P. Rasmussen, X. Rui, and J. E. Shield, Appl. Phys. Lett. **86**, 191915 (2005).
[16] C. P. Luo, S. H. Liou, L. Gao, Y. Liu, and D. J. Sellmyer, Appl. Phys. Lett. **77**, 2225 (2000).
[17] M. L. Yan, H. Zeng, N. Powers, and D. J. Sellmyer, J. Appl. Phys. **91**, 8471 (2002).
[18] H. Zeng, R. Sabirianov, O. Mryasov, M. L. Yan, K. Cho, and D. J. Sellmyer, Phys. Rev. B **66**, 184425 (2002).
[19] M. Luis, F. Nascimentoa, and C. Aparicio, Physica B **398**, 71 (2007).
[20] K. Tanaka, T. Ichitsubo, M. Amano, M. Koiwa, and K. Watanabe, Mater. Trans., JIM **41**, 917 (2000).
[21] T. Ichitsubo, M. Nakamoto, K. Tanaka, and M. Koiwa, Mater. Trans., JIM **39**, 24 (1998).
[22] T. Ichitsubo, K. Tanaka, M. Koiwa, and Y. Yamazaki, Phys. Rev. B **62**, 5435 (2000).
[23] K. Tanaka, T. Ichitsubo, and M. Koiwa, Mater. Sci. Eng., A **312**, 118 (2001).
[24] T. Ichitsubo, M. Koujina, M. Kawashima, and M. Hirao, Jpn. J. Appl. Phys., Part 1 **42**, 2858 (2003).
[25] T. Ichitsubo, K. Tanaka, M. Koujina, M. Kawashima, and M. Hirao, Jpn. J. Appl. Phys., Part 1 **43**, 273 (2004).
[26] K. Watanabe, S. Awaji, and K. Kimura, Jpn. J. Appl. Phys., Part 2 **36**, L673 (1997).
[27] H. Y. Wang, X. K. Ma, Y. J. He, S. Mitani, and M. Motokawa, Appl. Phys. Lett. **85**, 2304 (2004).
[28] T. Mura, *Micromechanics of Defects in Solids*, 2nd ed., revised (Martinus Nijhoff, The Hague, 1987).
[29] T. Ichitsubo and K. Tanaka, J. Appl. Phys. **96**, 6220 (2004).
[30] The data of the elastic constants of $L1_0$ FePt are unavailable. However, according to the data of FePd (Ref. 29), the elastic constants of the ordered phase are not so different from those of the disordered cubic phase. Therefore, this assumption is considered valid.